



AIAA 2003-5495

**LPV Antiwindup Compensation for
Enhanced Flight Control Performance**

Bei Lu and Fen Wu

Dept. of Mechanical and Aerospace Engineering

North Carolina State University

Raleigh, NC 27695

SungWan Kim

Dynamics and Control Branch

NASA Langley Research Center

Hampton, VA 23681-2199

**AIAA Guidance, Navigation, and Control
Conference**

August 11-14, 2003/Austin, TX

LPV Antiwindup Compensation for Enhanced Flight Control Performance

Bei Lu and Fen Wu*

*Dept. of Mechanical and Aerospace Engineering
North Carolina State University
Raleigh, NC 27695*

SungWan Kim[†]

*Dynamics and Control Branch
NASA Langley Research Center
Hampton, VA 23681-2199*

In this paper, we propose a saturation control scheme for linear parameter-varying (LPV) systems from an antiwindup control perspective. The proposed control approach is advantageous because it can be thought of as an augmented control algorithm from the existing control system. Moreover, the synthesis condition for an antiwindup compensator is formulated as a linear matrix inequality (LMI) optimization problem and can be solved efficiently. We have applied the LPV antiwindup controller to an F-16 longitudinal autopilot control system design to enhance aircraft safety and improve flight quality in a high angle of attack region.

Introduction

THE flight control system of a tactical aircraft has different performance goals for low angle of attack and high angle of attack regions. For example, in a low angle of attack scenario, pilots desire fast and accurate responses for maneuver and attitude tracking, whereas in a high angle of attack region, the flight control emphasis lies in the maintainability of aircraft stability with acceptable flying qualities. The potential of high angle of attack flight presents many challenges to the control designers. Due to aerodynamic surface saturation and control surface effectiveness, unconventional actuators such as thrust vectoring are suggested for aircraft maneuvering at and beyond the stall angle of attack. However, incorporation of additional thrust vectoring hardware could complicate the design of flight control laws in the poststall regime.¹ Robust multivariable control methods have been recently applied to a variety of aircraft models² to demonstrate their abilities to fly at high angles of attack (see Ref. 3 and references therein). Besides control law design, another major issue of high angle of attack flight is control saturation. It is well recognized that actuator saturation degrades the performance of the flight control system and may even lead to instability. The destabilizing effects of actuator saturation have been

cited as contributing factors in several mishaps involving high performance aircraft.⁴ For this reason, various methods of preventing instability due to saturation have been examined, which include allocating control effectors and command scaling and prioritization.

A popular approach to control saturation is the antiwindup method that employs a two-step design procedure. The main idea of antiwindup control is to design the linear controller ignoring the saturation nonlinearities first and then add antiwindup compensation to minimize adverse effects of the saturation on closed-loop performance. Desirable design requirements for antiwindup compensation subject to actuator saturation are the closed-loop system stability, recovery of the linear design specifications in the absence of saturation (linear performance recovery), and the smooth degradation of the linear performance in the presence of saturation (graceful performance degradation). Like other saturation control techniques, the antiwindup compensator design often assumes a linear time-invariant (LTI) plant and models the saturation block as a sector-bounded nonlinearity. Then absolute stability conditions (such as Popov, circle theorems) are applied for the stability and performance analysis.⁵

A general framework that unifies a large class of existing antiwindup control schemes in terms of two matrix parameters was proposed in Ref. 6. This framework is useful for understanding different antiwindup control schemes and motivates the development of systematic procedures for designing antiwindup controllers that provide guaranteed stability and perfor-

*Corresponding author, Assistant Professor, AIAA Member. E-mail: fwu@eos.ncsu.edu, Phone: (919) 515-5268, Fax: (919) 515-7968. This research was supported by Grant from NASA Langley Research Center (NAG-1-01119).

[†]Research Engineer, AIAA Associate Fellow.

Copyright © 2003 by Fen Wu. Published by the American Institute of Aeronautics and Astronautics, Inc. with permission.

mance. Early results in antiwindup control often have the drawback of lacking rigorous stability analysis and clear exposition of performance objectives. Using an extended circle criterion, the synthesis condition of static antiwindup controllers is formulated as a linear matrix inequality (LMI) problem in Ref. 7. A recent study in Ref. 8 has further revealed that antiwindup control for stable open-loop LTI systems can be solved *globally* as an LMI problem with the order of antiwindup compensator no more than the plant's order. Alternatively, the Popov stability condition has also been applied to the antiwindup compensator design problem.⁹ However, the synthesis condition of the saturation controller is given in coupled Riccati equations, which is difficult to solve for its optimal solution. Most previous antiwindup compensator designs are only applicable to open-loop stable LTI systems, limiting their usefulness for practical problems. When the system is nonlinear and open-loop unstable, the control synthesis problem becomes very difficult to solve, therefore, global stabilization cannot be achieved.^{10,11} However, in many control systems including flight control systems, the system dynamics are inherently nonlinear and their linearizations are strictly unstable.

The motivation for this research is twofold. First, the antiwindup control scheme for LTI plants in Ref. 12 is generalized to linear parameter-varying (LPV) systems. This generalization is very important because of the relevance of LPV systems to nonlinear systems. In fact, the LPV model can be thought of as a group of local descriptions of nonlinear dynamics. The antiwindup compensation augments existing control systems by maintaining stability and recovering control performance when actuator saturated. Second, saturation control for aircraft under large maneuver operations is critical due to safety concerns. The proposed antiwindup compensation can be developed by augmenting existing flight control algorithms. The consequence is enhanced reliability and an expanded flight envelope. In particular, we demonstrate adequate flight control performance using LPV antiwindup control in a high angle of attack scenario.

The notation in this paper is standard. \mathbf{R} stands for the set of real numbers and \mathbf{R}_+ for the non-negative real numbers. $\mathbf{R}^{m \times n}$ is the set of real $m \times n$ matrices. The transpose of a real matrix M is denoted by M^T . $\text{Ker}(M)$ is used to denote the orthogonal complement of M . A block diagonal matrix with submatrices X_1, X_2, \dots, X_p in its diagonal is denoted by $\text{diag}\{X_1, X_2, \dots, X_p\}$. We use $\mathbf{S}^{n \times n}$ to denote the real symmetric $n \times n$ matrices and $\mathbf{S}_+^{n \times n}$ to denote positive definite matrices. If $M \in \mathbf{S}^{n \times n}$, then $M > 0$ ($M \geq 0$) indicates that M is positive definite (positive semidefinite) and $M < 0$ ($M \leq 0$) denotes a negative definite (negative semidefinite) matrix. If $a, b \in \mathbf{R}$, then $\text{sect}[a, b]$ denotes the conic sector defined by $\{(q, p) : (p - aq)(p - bq) \leq 0\}$. For $x \in \mathbf{R}^n$,

its norm is defined as $\|x\| := (x^T x)^{\frac{1}{2}}$. The space of square integrable functions is denoted by \mathcal{L}_2 , that is, for any $u \in \mathcal{L}_2$, $\|u\|_2 := [\int_0^\infty u^T(t)u(t)dt]^{\frac{1}{2}}$ is finite.

LPV Antiwindup Control Synthesis

Antiwindup compensation is to modify nominal controllers so that if the signal from the controller is different from what enters the plant, corrective feedback action is employed to reduce the discrepancy. Because it is impossible to provide a global stabilizing solution to the antiwindup control problem when the open-loop plant is unstable, one often needs to determine regional stability for saturation control and to design controller gain in the guaranteed stability region.^{10,11} In Ref. 8, a sector-bounded input nonlinearity, $\text{sect}[0, 1]$, was considered for the open-loop stable plant and is not applicable to exponentially unstable systems. However, the derived performance and stability properties can be improved when the input nonlinearity is restricted to a smaller sector region. As a result, this modification leads to regional stability of the antiwindup compensated system and extends the antiwindup control technique to exponentially unstable open-loop systems.

Consider an LPV plant P_ρ described by

$$\begin{bmatrix} \dot{x}_p \\ e \\ y \end{bmatrix} = \begin{bmatrix} A_p(\rho) & B_{p1}(\rho) & B_{p2}(\rho) \\ C_{p1}(\rho) & D_{p11}(\rho) & D_{p12}(\rho) \\ C_{p2}(\rho) & D_{p21}(\rho) & D_{p22}(\rho) \end{bmatrix} \begin{bmatrix} x_p \\ d \\ \sigma(u) \end{bmatrix} \quad (1)$$

where the plant state $x_p \in \mathbf{R}^{n_p}$. $y \in \mathbf{R}^{n_y}$ is the measurement for control, and $\sigma(u) \in \mathbf{R}^{n_u}$ is the saturated control input. $e \in \mathbf{R}^{n_e}$ is the controlled output and $d \in \mathbf{R}^{n_d}$ is the disturbance input. It is assumed that the vector-valued parameter ρ evolves continuously over time and its range is limited to a compact subset $\mathcal{P} \subset \mathbf{R}^s$. In addition, its time derivative is assumed to be bounded and satisfy the constraint $\underline{v}_i \leq \dot{\rho}_i \leq \bar{v}_i, i = 1, 2, \dots, s$. For notational purposes, denote $\mathcal{V} = \{v : \underline{v}_i \leq v \leq \bar{v}_i, i = 1, 2, \dots, s\}$, where \mathcal{V} is a given convex polytope in \mathbf{R}^s that contains the origin. Given the sets \mathcal{P} and \mathcal{V} , the parameter ν -variation set is defined as

$$\mathcal{F}_\mathcal{P}^\mathcal{V} = \{\rho \in C^1(\mathbf{R}_+, \mathbf{R}^s) : \rho(t) \in \mathcal{P}, \dot{\rho}(t) \in \mathcal{V}, \forall t \geq 0\}$$

So $\mathcal{F}_\mathcal{P}^\mathcal{V}$ specifies the set of all allowable parameter trajectories. In the interests of notational compactness, the parameter dependence will not always be shown from now on.

All matrix valued state-space data are continuous and have appropriate dimensions. For simplicity, we assume that

- (A1) (A_p, B_{p2}, C_{p2}) triple is parameter-dependent stabilizable and detectable for all ρ . The LPV system (1) is said to be parameter-dependent stabilizable if there exists continuously differentiable

matrix functions $X(\rho) = X^T(\rho) > 0$ and $F(\rho)$, such that for $(\rho, \dot{\rho}) \in \mathcal{P} \times \mathcal{V}$

$$(A_p + B_{p2}F)^T X + X(A_p + B_{p2}F) + \sum_{i=1}^s \dot{\rho}_i \frac{\partial X}{\partial \rho_i} < 0$$

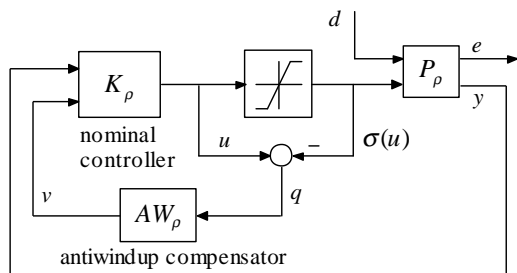
(A2) The matrices $\begin{bmatrix} B_{p2}^T & D_{p12}^T \end{bmatrix}$ and $\begin{bmatrix} C_{p2} & D_{p21} \end{bmatrix}$ have full row rank.

(A3) $D_{p22} = 0$.

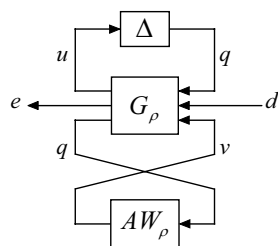
The actuator nonlinearity under consideration is a piecewise-linear saturation

$$\sigma(u_i) = \begin{cases} u_i & |u_i| \leq u_i^{\max} \\ \text{sgn}(u_i)u_i^{\max} & |u_i| > u_i^{\max} \end{cases}$$

for $i = 1, 2, \dots, n_u$. The antiwindup control structure is shown in Fig. 1(a).



(a) LPV antiwindup controller structure



(b) Equivalent transformation

Fig. 1 Nonlinear saturation control diagram.

Following the standard antiwindup procedure, a nominal LPV controller K_ρ is designed first by ignoring the input nonlinearity. Different linear control design techniques can be employed to achieve this goal. A systematic way to do this is through LPV control theory.^{13–15} Due to the assumption **(A1)**, the nominal controller K_ρ is capable of stabilizing the open-loop system when no input saturation exists, and its design will determine the nominal performance of the closed-loop LPV system. We assume that such a controller is given by

$$\begin{bmatrix} \dot{x}_k \\ u \end{bmatrix} = \begin{bmatrix} A_k(\rho, \dot{\rho}) & B_k(\rho) \\ C_k(\rho) & D_k(\rho) \end{bmatrix} \begin{bmatrix} x_k \\ y \end{bmatrix} + \begin{bmatrix} v_1 \\ v_2 \end{bmatrix} \quad (2)$$

where $x_k \in \mathbf{R}^{n_k}$. The variables v_1, v_2 are the auxiliary inputs provided by an antiwindup compensator. They

are used to condition the nominal controller when the control input is saturated.

Our objective is to design an LPV antiwindup compensator AW_ρ such that the adverse effect of input saturations are minimized in terms of induced \mathcal{L}_2 norm. The antiwindup compensator is in the form of

$$\begin{bmatrix} \dot{x}_{aw} \\ v_1 \\ v_2 \end{bmatrix} = \begin{bmatrix} A_{aw}(\rho, \dot{\rho}) & B_{aw}(\rho) \\ C_{aw}(\rho, \dot{\rho}) & D_{aw}(\rho) \end{bmatrix} \begin{bmatrix} x_{aw} \\ q \end{bmatrix} \quad (3)$$

where the state $x_{aw} \in \mathbf{R}^{n_{aw}}$; the size of the compensator state is determined later on. Such antiwindup compensation schemes provide a computationally efficient technique for the “retro-fitting” existing unconstrained controller K_ρ to account for input nonlinearities, thereby eliminating controller windup problems for input saturated nonlinear systems.

The LPV antiwindup control diagram in Fig. 1(a) can be transformed to its equivalent form by substituting the actuator saturation with a deadband nonlinearity $\Delta_i = 1 - \frac{\sigma(u_i)}{u_i}$ and $\Delta = \text{diag}\{\Delta_1, \Delta_2, \dots, \Delta_{n_u}\}$, as shown in Fig. 1(b). This allows recasting of the compensator design problem into a robust control paradigm.

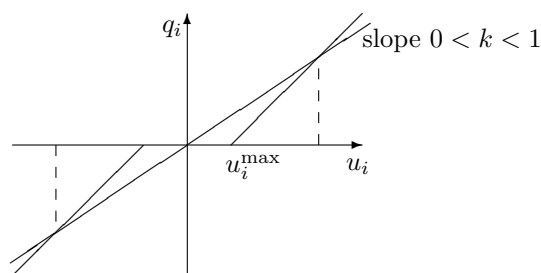


Fig. 2 Restricted range input saturation.

It can be seen that the deadband uncertainty Δ_i resides in the conic sector $[0, 1]$. The magnitude of the control input signal u_i is restricted to be less than $\left(\frac{1}{1-k}\right)u_i^{\max}$ by reducing the nonlinearity Δ_i to $\text{sect}[0, k]$ with $0 < k < 1$. Consequently, we have $\Delta \in \text{sect}[0, kI]$. The resulting stability notion then becomes regional stability. However, this restriction of uncertainty Δ extends the antiwindup scheme to open-loop exponentially unstable systems.

Let the system G_ρ be the interconnection of the open-loop system P_ρ and the nominal controller K_ρ , but exclude the antiwindup compensator. Then its dynamic equation is

$$\begin{bmatrix} \dot{x} \\ u \\ e \\ q \end{bmatrix} = \begin{bmatrix} A(\rho, \dot{\rho}) & B_0(\rho) & B_1(\rho) & B_2(\rho) \\ C_0(\rho) & D_{00}(\rho) & D_{01}(\rho) & D_{02}(\rho) \\ C_1(\rho) & D_{10}(\rho) & D_{11}(\rho) & D_{12}(\rho) \\ 0 & I & 0 & 0 \end{bmatrix} \begin{bmatrix} x \\ q \\ d \\ v_1 \\ v_2 \end{bmatrix} \quad (4)$$

$$q = \Delta u \quad (5)$$

antiwindup controller, the resulting synthesis condition is convex in terms of matrix variables R_{11}, S , and V . In fact, the solvability condition for the LPV antiwindup compensator is provided as an infinite-dimensional LMI optimization problem, for which an efficient numerical algorithm exists to solve it approximately.¹⁷ This can be done by parameterizing the matrix variables using a finite set of scalar basis functions as

$$R_{11}(\rho) = \sum_{i=1}^{N_f} f_i(\rho) R_{11,i} \quad S(\rho) = \sum_{j=1}^{N_g} g_j(\rho) S_j$$

$$V(\rho) = \sum_{k=1}^{N_h} h_k(\rho) V_k$$

where $\{f_i(\rho)\}_{i=1}^{N_f}$, $\{g_j(\rho)\}_{j=1}^{N_g}$ and $\{h_k(\rho)\}_{k=1}^{N_h}$ are user-specified scalar basis functions. $R_{11,i}, S_j$, and V_k are new optimization variables to be determined. After such a parameterization, the LPV synthesis conditions can be solved using a gridding method over the parameter space.

After solving R_{11}, S , and V matrix functions, the LPV antiwindup compensator gain can be determined by either solving the feasibility problem from the closed-loop LMI (13) or the antiwindup compensator can be constructed explicitly as shown in the following theorem. The explicit construction approach is advantageous because it avoids possible numerical ill-condition when solving the above feasibility LMI problem. Moreover, it connects the antiwindup controller directly to the plant and nominal controller gains.

Theorem 2 (*LPV Antiwindup Compensator Construction*)

Given the solutions R_{11}, S, γ and $V = W^{-1}$ of the LMIs (9)–(11), let $MN^T = I_n - RS$ with $M, N \in \mathbf{S}^{n \times n_p}$ and $E^T = [I_{n_p} \ 0]$, then one n_p -th order LPV antiwindup compensator AW_ρ can be constructed through the following scheme:

1. Compute a feasible $\hat{D}_{aw}(\rho) \in \mathbf{R}^{n_u \times n_u}$ such that

$$\begin{bmatrix} -k(W\hat{D}_{aw} + \hat{D}_{aw}^T W) + 2W & * & * \\ -kD_{01}^T W & \gamma I_{n_d} & * \\ -(D_{10} + D_{p12}\hat{D}_{aw}) & -D_{11} & \gamma I_{n_e} \end{bmatrix} > 0$$

for all $\rho \in \mathcal{P}$. Denote the above inequality as $\Pi(\rho)$.

2. Compute the least square solutions of the following linear equations for $\hat{B}_{aw}(\rho) \in \mathbf{R}^{n \times n_u}, \hat{C}_{aw}(\rho) \in$

$\mathbf{R}^{n_u \times n_p}$

$$\begin{bmatrix} 0 & I_{n_u} & 0 & 0 \\ I_{n_u} & & & \\ 0 & & -\Pi & \\ 0 & & & \end{bmatrix} \begin{bmatrix} \hat{B}_{aw}^T \\ ? \end{bmatrix}$$

$$= - \begin{bmatrix} 0_{n_u \times n} \\ B_0^T S + kW C_0 \\ B_1^T S \\ C_1 \end{bmatrix}$$

$$\begin{bmatrix} 0 & kW^T & 0 & D_{p12}^T \\ kW & & & \\ 0 & & -\Pi & \\ D_{p12} & & & \end{bmatrix} \begin{bmatrix} \hat{C}_{aw} \\ ? \end{bmatrix}$$

$$= - \begin{bmatrix} B_{p2}^T \\ (B_0^T + kW C_0 R E + \hat{D}_{aw}^T B_{p2}^T) \\ B_1^T E \\ C_1 R E \end{bmatrix}$$

and the matrix $\hat{A}_{aw}(\rho, \dot{\rho}) \in \mathbf{R}^{n \times n_p}$ as

$$\hat{A}_{aw} = -\dot{\rho} \frac{dS}{d\rho} R E - \dot{\rho} \frac{dN}{d\rho} M^T E - A^T E$$

$$- [S B_0 + \hat{B}_{aw} + k C_0^T W \quad S B_1 \quad C_1^T] \Pi^{-1}$$

$$\times \begin{bmatrix} (B_0^T + kW C_0 R) E + \hat{D}_{aw}^T B_{p2}^T + kW \hat{C}_{aw} \\ B_1^T E \\ C_1 R E + D_{p12} \hat{C}_{aw} \end{bmatrix}$$

3. Convert the transformed antiwindup compensator gain to its original state-space data by

$$\begin{bmatrix} A_{aw} & B_{aw} \\ C_{aw} & D_{aw} \end{bmatrix} = \begin{bmatrix} N & S B_2 \\ 0 & [0 \quad I_{n_u}] \end{bmatrix}^{-1}$$

$$\times \left(\begin{bmatrix} \hat{A}_{aw} & \hat{B}_{aw} \\ \hat{C}_{aw} & \hat{D}_{aw} \end{bmatrix} - \begin{bmatrix} S A R E & 0 \\ 0 & 0_{n_u \times n_u} \end{bmatrix} \right)$$

$$\times \begin{bmatrix} M^T E & 0 \\ 0 & I_{n_u} \end{bmatrix}^{-1}$$

Proof: The derivation of the antiwindup controller formula basically follows the procedure outlined in Ref. 12. Define

$$Z_1 = \begin{bmatrix} I & R E \\ 0 & M^T E \end{bmatrix}, \quad Z_2 = \begin{bmatrix} S & E \\ N^T & 0 \end{bmatrix}$$

Then it can be shown that $X_{cl} Z_1 = Z_2$. Also we have the following congruent transformation:

$$Z_1^T X_{cl} Z_1 = \begin{bmatrix} S & E \\ E^T & E^T R E \end{bmatrix}$$

$$Z_1^T \frac{dX_{cl}}{dt} Z_1 = \begin{bmatrix} \frac{dS}{dt} & (R \frac{dS}{dt} + M \frac{dN^T}{dt})^T E \\ E^T (R \frac{dS}{dt} + M \frac{dN^T}{dt}) & -E^T \frac{dR}{dt} E \end{bmatrix}$$

$$\begin{aligned}
& \begin{bmatrix} Z_1^T X_{cl} A_{cl} Z_1 & Z_1^T X_{cl} B_{0,cl} & Z_1^T X_{cl} B_{1,cl} \\ C_{0,cl} Z_1 & D_{00,cl} & D_{01,cl} \\ C_{1,cl} Z_1 & D_{10,cl} & D_{11,cl} \end{bmatrix} \\
&= \begin{bmatrix} SA & 0 & SB_0 & SB_1 \\ E^T A & E^T ARE & E^T B_0 & E^T B_1 \\ C_0 & C_0 RE & D_{00} & D_{01} \\ C_1 & C_1 RE & D_{10} & D_{11} \end{bmatrix} \\
&+ \begin{bmatrix} I_n & 0 \\ 0 & B_{p2} \\ 0 & I \\ 0 & D_{p12} \end{bmatrix} \begin{bmatrix} \hat{A}_{aw} & \hat{B}_{aw} \\ \hat{C}_{aw} & \hat{D}_{aw} \end{bmatrix} \begin{bmatrix} 0 & I_{n_p} & 0 & 0 \\ 0 & 0 & I & 0 \end{bmatrix}
\end{aligned}$$

where

$$\begin{aligned}
\begin{bmatrix} \hat{A}_{aw} & \hat{B}_{aw} \\ \hat{C}_{aw} & \hat{D}_{aw} \end{bmatrix} &= \begin{bmatrix} SARE & 0 \\ 0 & 0 \end{bmatrix} \\
&+ \begin{bmatrix} N & SB_2 \\ 0 & [0 \ I] \end{bmatrix} \begin{bmatrix} A_{aw} & B_{aw} \\ C_{aw} & D_{aw} \end{bmatrix} \begin{bmatrix} M^T E & 0 \\ 0 & I \end{bmatrix}
\end{aligned}$$

Multiply $\text{diag}\{Z_1^T, I, I, I\}$ from the left side and its conjugate transpose from the right side of eq. (13), and we get

$$\begin{bmatrix} H_{11} & * & * \\ H_{21} & H_{22} & * \\ L_1 & L_2 & -\Pi \end{bmatrix} < 0 \quad (18)$$

with the shorthand notation

$$\begin{aligned}
H_{11} &= SA + A^T S + \sum_{i=1}^s \dot{\rho}_i \frac{\partial S}{\partial \rho_i} \\
H_{21} &= E^T A + \hat{A}_{aw}^T + E^T (R \frac{dS}{dt} + M \frac{dN^T}{dt}) \\
H_{22} &= E^T (AR + RA^T - \sum_{i=1}^s \dot{\rho}_i \frac{\partial R}{\partial \rho_i}) E \\
&+ B_{p2} \hat{C}_{aw} + \hat{C}_{aw}^T B_{p2}^T \\
L_1 &= \begin{bmatrix} B_0^T S + \hat{B}_{aw}^T + kW C_0 \\ B_1^T S \\ C_1 \end{bmatrix} \\
L_2 &= \begin{bmatrix} (B_0^T + kW C_0 R) E + \hat{D}_{aw}^T B_{p2}^T + kW \hat{C}_{aw} \\ B_1^T E \\ C_1 R E + D_{p12} \hat{C}_{aw} \end{bmatrix}
\end{aligned}$$

By Schur complement, it is equivalent to

$$\begin{bmatrix} H_{11} + L_1^T \Pi^{-1} L_1 & * \\ H_{21} + L_2^T \Pi^{-1} L_1 & H_{22} + L_2^T \Pi^{-1} L_2 \end{bmatrix} < 0 \quad (19)$$

Clearly, the lower (3×3) matrix of the inequality (18) must be negative definite, this determines the feasible \hat{D}_{aw} . Let the $(2, 1)$ element be equal to zeros and one can solve for \hat{A}_{aw} . This also leads to decoupled LMIs from the inequality (19). Then $\hat{B}_{aw}, \hat{C}_{aw}$ terms can be solved from the $(1, 1)$ and $(2, 2)$ elements of the decoupled inequality (19). Note that both inequalities have regular solutions.¹⁸

The $(1, 1)$ element of the above matrix inequality corresponds to LMI (10) after elimination of the variables \hat{B}_{aw} and \hat{D}_{aw} . It can also be shown that the $(2, 2)$ element is equivalent to LMI (9) by eliminating $\hat{C}_{aw}, \hat{D}_{aw}$. *Q.E.D.*

The explicit antiwindup construction scheme can also be applied to open-loop stable systems. However, because the synthesis condition for an open-loop stable plant does not involve matrix W ,⁸ we need to solve the feasible \hat{D}_{aw} and W matrices altogether at the first step. The remaining steps are the same by setting $k = 1$.

Saturation Control for Flight Dynamics

In this section, the proposed LPV antiwindup control synthesis technique is applied to flight dynamics. The system to be controlled is the longitudinal F-16 aircraft model based on NASA Langley Research Center (LaRC) wind tunnel tests,¹⁹ which is described by Stevens and Lewis in great detail.²⁰ The full nonlinear longitudinal model of an F-16 aircraft is given as follows:

$$\begin{aligned}
\dot{V} &= \frac{\bar{q} S \bar{c}}{2mV} [C_{xq} \cos \alpha + C_{zq} \sin \alpha] q + T \frac{\cos \alpha}{m} \\
&- g \sin(\theta - \alpha) + \frac{\bar{q} S}{m} [C_z \cos \alpha + C_z \sin \alpha] \quad (20)
\end{aligned}$$

$$\begin{aligned}
\dot{\alpha} &= \left[1 + \frac{\bar{q} S \bar{c}}{2mV^2} (C_{zq} \cos \alpha - C_{xq} \sin \alpha) \right] q - T \frac{\sin \alpha}{mV} \\
&+ \frac{g}{V} \cos(\theta - \alpha) + \frac{\bar{q} S}{mV} [C_z \cos \alpha - C_x \sin \alpha] \quad (21)
\end{aligned}$$

$$\dot{q} = \frac{\bar{q} S \bar{c}}{2I_y V} [\bar{c} C_{mq} + \Delta C_{zq}] q + \frac{\bar{q} S \bar{c}}{I_y} \left[C_m + \frac{\Delta}{\bar{c}} C_z \right] \quad (22)$$

$$\dot{\theta} = q \quad (23)$$

The aerodynamic coefficients are provided as lookup tables from NASA LaRC wind tunnel tests on a scale model of F-16 aircraft. The data apply to the speed range up to about Mach 0.6, and cover a very wide range of angle of attack ($-20^\circ \leq \alpha \leq 90^\circ$). However, conventional aerodynamic math models for use in aircraft simulation or flight control design have become increasingly deficient in the poststall region. So, the investigation on the robust control of aircraft in the high angle of attack region with uncertain aerodynamic coefficients is one of the challenging research topics.

The F-16 is powered by an afterburning turbofan jet engine, which produces a thrust force in the x axis. The NASA data include a model of the engine in which the thrust response is modeled with a first-order lag; the lag time constant is a function of the actual engine power level and the commanded power. The throttle position is related to the commanded power level. For

convenience, the actual power level is also considered as a state variable in longitudinal dynamics.

The nonlinear model is then linearized at trim conditions to generate state-space models for design. The state and input variables are as follows:

$$x = \begin{cases} V & \text{true airspeed (ft/s)} \\ \alpha & \text{angle of attack (rad)} \\ q & \text{pitch rate (rad/s)} \\ \theta & \text{pitch angle (rad)} \\ \text{pow} & \text{actual power level (0-100)} \end{cases}$$

$$u = \begin{cases} \delta_{th} & \text{throttle position (0-1)} \\ \delta_e & \text{elevator angle (deg) } (-25^\circ-25^\circ) \end{cases}$$

By slight abuse of notations, the above listed variables are perturbations from their equilibrium states. In addition, V , q , and flight path angle γ are selected as outputs. The operating envelope of interest covers aircraft speeds between 160 ft/s and 200 ft/s and angles of attack between 20° and 45° . These two variables are used as scheduling parameters in the LPV modeling of F-16 longitudinal dynamics. Fig. 3 shows the flight trim points for the control design. The corresponding dynamic pressure of the designed range is between 20 psf and 50 psf. This portion of flight envelope is chosen because the moderately high angle of attack and the low dynamic pressure cause aerodynamic control surface saturation.

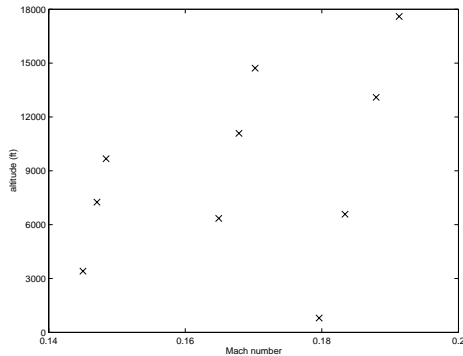


Fig. 3 Flight trim points.

The design objective of the nominal LPV controller in this research is to track the flight path angle command with the tracking error about 1.25% of the command in the steady state. This kind of problem is formulated as a model-following problem,^{21,22} where the ideal model to be followed is chosen to be a second-order filter based on desired flying qualities

$$\frac{\gamma_{ideal}}{\gamma_{cmd}} = \frac{\omega_{ideal}^2}{s^2 + 2\zeta_{ideal}\omega_{ideal}s + \omega_{ideal}^2} \quad (24)$$

The implicit model-following framework allows for direct incorporation of flying quality specifications into the control design. A block diagram of the system interconnection structure for synthesizing the nominal controller is shown in Fig. 4.

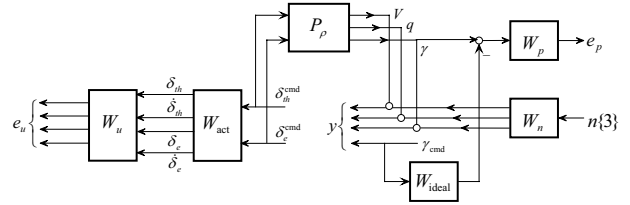


Fig. 4 Open-loop interconnection for LPV control design.

The weighting functions are chosen as

$$W_p = \frac{80(s/5 + 1)}{s/0.05 + 1}$$

$$W_n = \text{diag}\{0.8, 0.6, 0.1\}$$

$$W_u = \text{diag}\left\{1, 10, \frac{1}{50}, \frac{1}{120}\right\}$$

$$W_{ideal} = \frac{2.25}{s^2 + 2.4s + 2.25}$$

The throttle and elevator actuator dynamics are modeled as first order filters.

$$\frac{\delta_{th}}{\delta_{th}^{cmd}} = \frac{5}{s + 5} \quad \frac{\delta_e}{\delta_e^{cmd}} = \frac{20}{s + 20}$$

Both the position and the rate of control inputs are fed into W_u to penalize the control effort. Therefore, the system matrix of W_{act} is derived as follows.

$$W_{act} = \text{diag}\left\{\left[\frac{5}{s+5}\right], \left[\frac{20}{s+20}\right]\right\}$$

The nominal controller is designed by formulating an LPV synthesis problem, which can be solved using either a single or parameter-dependent quadratic Lyapunov function over all gridding points in the two dimensional parameter space.^{13,14} In this work, the single quadratic Lyapunov function (SQLF) approach is chosen to reduce the computation time in the nominal LPV control synthesis phase. The performance obtained through the SQLF approach is $\gamma_{nom} = 8.0$.

The nonlinear F-16 longitudinal dynamics with the nominal LPV controller K_p is simulated, and the magnitude limits of actuators are enforced during the simulation. One designed flight condition is used as the test point, which is a trimmed flight at $V = 160$ ft/s and $\alpha = 35^\circ$. Figures 5 and 6 show the nonlinear time responses of the aircraft model to the flight path doublet input with different magnitudes.

It is observed that when flight path doublet input is equal to $\pm 1^\circ$, the positions of throttle and elevator are not saturated. The simulation result of the flight path shows that the measurement matches the ideal response very well. For comparison, the nonlinear time response for a more drastic $\pm 2^\circ$ flight path doublet input is shown in Fig. 6. It should require

more control actions of the actuators to achieve the performance objective. Unfortunately, the elevator is saturated severely and thus makes the system unstable.

The proposed LPV antiwindup scheme is applied to the control of the F-16 aircraft, and we also choose the SQLF approach to perform the LPV synthesis. A series of LPV antiwindup compensators AW_ρ are designed by gradually decreasing k value from 1 to 0.90. Table 1 shows the corresponding performance level γ . Because one of the gridding points is unstable, the synthesis condition for LPV antiwindup control is infeasible for $k = 1$. Compared with the nominal performance, the worst performance level when $k = 1 - 10^{-5}$ indicates the strong adverse effect of saturation nonlinearity. When $k = 0.90$, the antiwindup compensator almost recovers the nominal closed-loop performance γ_{nom} .

Table 1 H_∞ performance level vs. sector range $[0, kI]$.

Sector range $[0, kI]$	\mathcal{H}_∞ performance γ
$1 - 10^{-5}$	1596.38
$1 - 10^{-4}$	258.30
$1 - 10^{-3}$	32.16
0.99	8.41
0.90	8.00

Now, a $\pm 2^\circ$ flight path command input is applied to the F-16 aircraft system with the antiwindup compensator. The time response of the nonlinear system at the same trimmed condition is tested. As shown in Fig. 7, the antiwindup compensator not only stabilizes the system when saturation occurs, but also provides fairly good recovery of tracking performance.

Conclusion

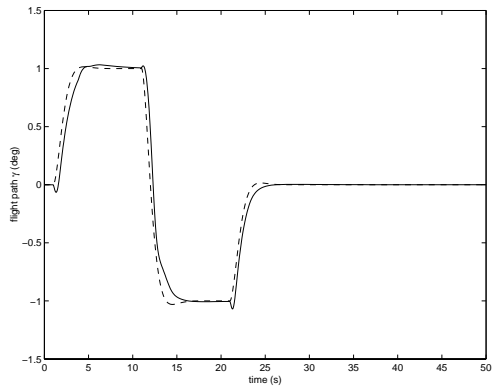
We have developed an antiwindup control scheme for LPV systems and applied the proposed saturation control scheme to F-16 aircraft. Due to the special structure of the antiwindup control scheme, the LPV antiwindup control synthesis condition is solvable by LMI optimizations. The extension of the antiwindup control idea to LPV systems provides a practical approach for nonlinear flight dynamics in the presence of actuator saturation. Saturation control is particularly important to near stall and poststall flight conditions. By augmenting the nominal longitudinal autopilot with antiwindup compensator, it was shown through nonlinear simulation that the F-16 aircraft maintains its stability and has adequate control performance in a high angle of attack. Applying antiwindup control scheme to flight control is promising because no additional actuator is needed to compensator control authority. In fact, the implementation of antiwindup controllers could be done by modifying flight control software.

Acknowledgment

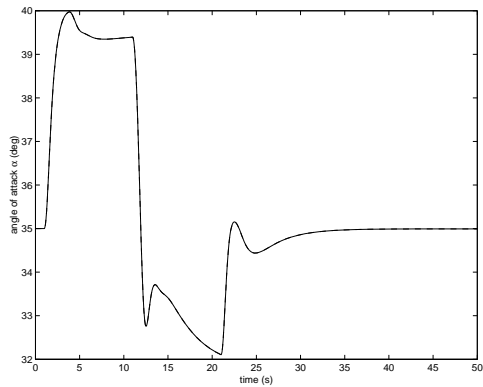
The first two authors would like to acknowledge the financial support for this research by NASA Langley Research Center under Grant NAG-1-01119.

References

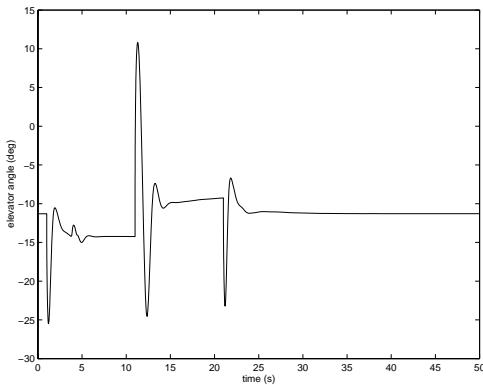
- ¹Reigelsperger, W.C. and Banda, S.S., "Nonlinear simulation for a modified F-16 with full-envelope control laws," *Contr. Eng. Practice*, 6:309–320, 1998.
- ²Balas, G.J., Doyle, J.C., Glover, K., Packard, A.K., and Smith, R., *μ -Analysis and Synthesis Toolbox*, Mathworks Inc., Natick, MA, 1991.
- ³Adams, R.J., Buffington, J.M., Sparks, A.G., and Banda, S.S., *Robust Multivariable Flight Control*, Springer-Verlag, London, UK, 1994.
- ⁴Dornheim, M.A., "Report pinpoints factors leading to YF-22 crash," *Aviation Week Space Technol.*, pp. 53–54, Nov. 9, 1992.
- ⁵Khalil, H.K., *Nonlinear Systems*, 2nd ed., Prentice-Hall, Englewood Cliffs, NJ, 1996.
- ⁶Kothare, M.V., Campo, P.J., Morari, M., and Nett, C.N., "A unified framework for the anti-windup designs," *Automatica*, 30(12):1869–1883, 1994.
- ⁷Mulder, E.F., Kothare, M.V., and Morari, M., "Multi-variable anti-windup controller synthesis using linear matrix inequalities," *Automatica*, 37:1407–1416, 2001.
- ⁸Grimm, G., Hatfield, J., Postlethwaite, I., Teel, A.R., Turner, M.C., and Zaccarian, L., "Anti-windup: An LMI-based synthesis," to appear in *IEEE Trans. Automat. Contr.*, 2003.
- ⁹Tyan, F. and Bernstein, D.S., "Anti-windup compensator synthesis for systems with saturation actuators," *Int. J. Robust Non. Contr.*, 5:521–537, 1995.
- ¹⁰Teel, A.R., "Anti-windup for exponentially unstable linear systems," *Int. J. Robust Non. Contr.*, 9:701–716, 1999.
- ¹¹Hu, T. and Lin, Z., *Control Systems with Actuator Saturation: Analysis and Design*, Birkhäuser, Boston, 2001.
- ¹²Wu, F. and Lu, B., "Anti-Windup Control Design for Exponentially Unstable LTI Systems with Actuator Saturation," to appear in *Proc. 2003 Amer. Contr. Conf.*, June 2003.
- ¹³Becker, G., and Packard, A., "Robust performance of linear parametrically varying systems using parametrically-dependent linear feedback," *Syst. Contr. Letts.*, 23:205–215, 1994.
- ¹⁴Wu, F., Yang, X.H., Packard, A., and Becker, G., "Induced \mathcal{L}_2 norm control for LPV systems with bounded parameter variation rates," *Int. J. Robust Non. Contr.*, 6(9/10):983–998, 1996.
- ¹⁵Apkarian, P., and Adams, R.J., "Advanced gain-scheduling techniques for uncertain system," *IEEE Trans. Contr. Syst. Tech.*, 6:21–32, 1998.
- ¹⁶Boyd, S.P., El Ghaoui, L., Feron, E., and Balakrishnan, V., *Linear Matrix Inequalities in Systems and Control Theory* SIAM, Philadelphia, PA, 1994.
- ¹⁷Gahinet, P., Nemirovskii, A., Laub, A.J., and Chilali, M., *LMI Control Toolbox* Mathworks, Natick, MA, 1995.
- ¹⁸Gahinet, P., "Explicit controller formulas for LMI-based \mathcal{H}_∞ synthesis," *Automatica*, 32(7):1007–1014, 1996.
- ¹⁹Nguyen, L.T., Ogburn, M.E., Gillert, W.P., Kibler, K.S., Brown, P.W., and Deal, P.L., "Simulator study of stall/post-stall characteristics of a fighter airplane with relaxed longitudinal static stability," *NASA Technical Paper* 1538, 1979.
- ²⁰Stevens, B.L. and Lewis, F.L., *Aircraft Control and Simulation*, John Wiley & Sons, Inc., 1992.
- ²¹Buffington, J.M., Sparks, A.G., and Banda, S.S., "Robust longitudinal axis flight control for an aircraft with thrust vectoring," *Automatica*, 30(10):1527–1540, 1994.
- ²²Shin, J.-Y., Balas, G.J., and Kaya, A.M., "Blending approach of linear parameter varying control synthesis for F-16 aircraft," *AIAA Paper No. 01-4040*, 2001.



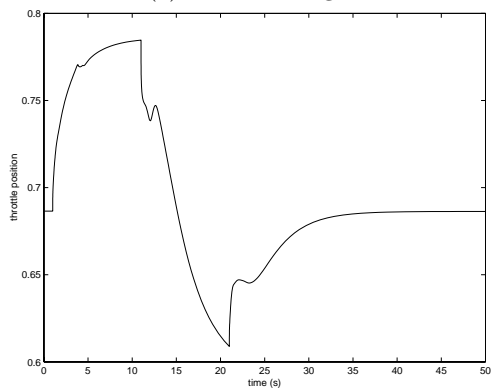
(a) Flight path angle



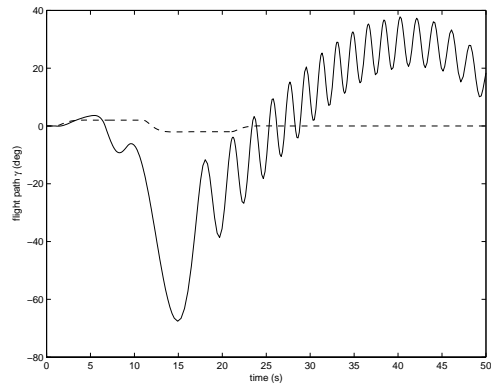
(b) Angle of attack



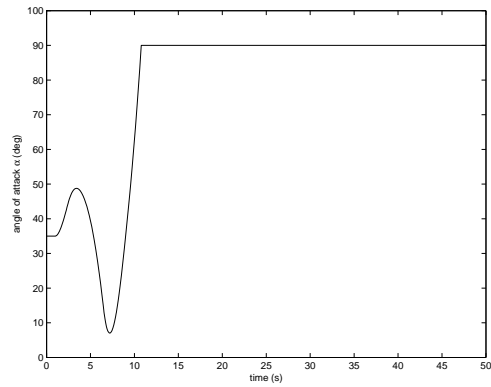
(c) Elevator angle



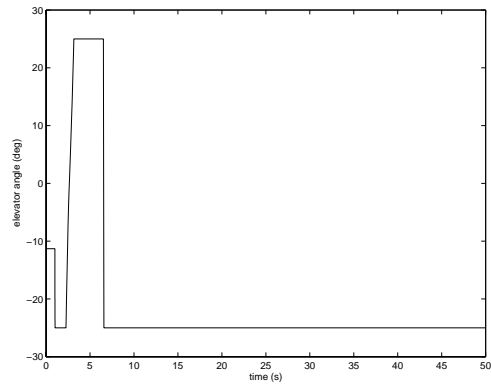
(d) Throttle position



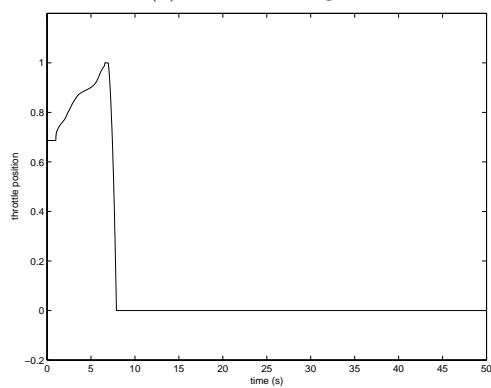
(a) Flight path angle



(b) Angle of attack



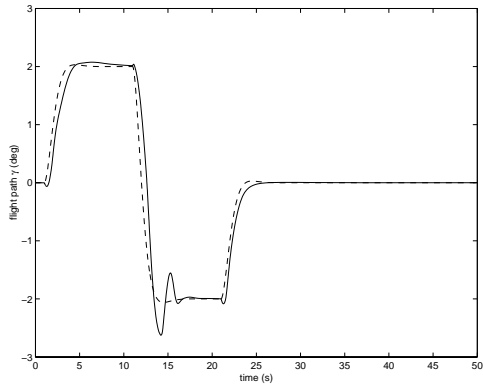
(c) Elevator angle



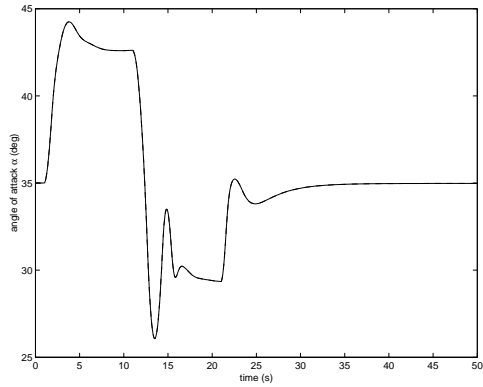
(d) Throttle position

Fig. 5 Nonlinear simulation of F-16 dynamics to $\pm 1^\circ$ flight path doublet input.

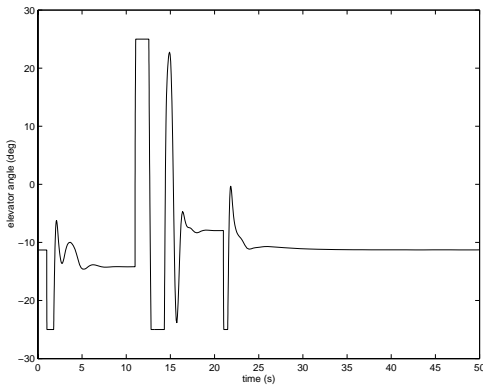
Fig. 6 Nonlinear simulation of F-16 dynamics to $\pm 2^\circ$ flight path doublet input.



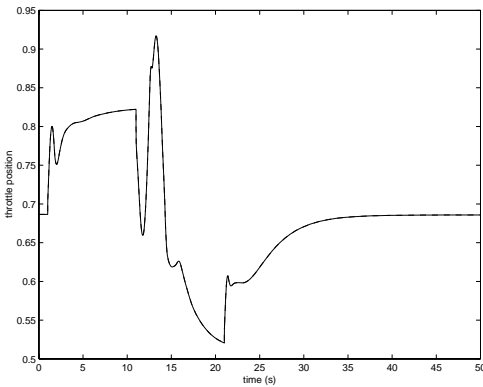
(a) Flight path angle



(b) Angle of attack



(c) Elevator angle



(d) Throttle position

Fig. 7 Saturation control of F-16 dynamics using LPV antiwindup compensator.